Tensile test of the main cement paste phases using molecular dynamics simulation

Sela Hoeun, Fabrice Bernard, Frederic Grondin, Siham Kamali-Bernard, Syed Yasir Alam

Tensile test of the main cement paste phases using molecular dynamics simulation

S. HOEUN[a,b], F. BERNARD[b], F. GRONDIN[a], S. KAMALI-BERNARD[b], S. Y ALAM[a]

a. Institut de Recherche en Génie Civil et Mécanique (GeM), UMR 6183 Centrale Nantes – Université de Nantes – CNRS, 1 rue de la Noë 44321 Nantes cedex 3, France ; sela.hoeun@ec-nantes.fr, frederic.grondin@ec-nantes.fr, syed-yasir.alam@ec-nantes.fr

b. Laboratoire de Génie Civil et Génie Mécanique (LGCGM), INSA Rennes, 20 avenue des Buttes de Coësmes 35700 Rennes, France ; fabrice.bernard@insa-rennes.fr, siham.kamali-bernard@insa-rennes.fr

Résumé :

De nos jours, la production de ciment est l'une des principales causes d'émission de dioxyde de carbone (CO_2), qui contribue à la cause du changement climatique. Cependant, le ciment reste l'un des principaux matériaux pour la construction de bâtiments en raison de son prix, de sa capacité à couler sous différentes formes selon les exigences de l'architecture et de sa résistance. En conséquence, il est nécessaire de développer la résistance de la pâte de ciment hydraté. D'une part, cela pourrait impliquer la durabilité et la pérennité de la structure. D'autre part, l'amélioration de la résistance pourrait conduire à une moindre utilisation de ciment, ce qui permet également de réduire la production de ciment. Afin de répondre à cette problématique, l'étude des propriétés mécaniques des nouvelles pâtes cimentaires est très importante, mais elle nécessite d'améliorer les connaissances à l'échelle nanométrique. L'une des méthodes consiste à utiliser des simulations de dynamique moléculaire. Cette méthode est assez populaire dans l'étude des propriétés mécaniques du ciment car il est fastidieux de réaliser l'échantillon pour l'expérimentation à si petite échelle. L'homogénéisation des propriétés de l'échelle nano à l'échelle micro n'est pas vraiment maîtrisée jusqu'à présent. Dans notre étude, nous avons effectué les tests de traction en utilisant la simulation de dynamique moléculaire afin de les trouver pour différents composants (c.-à-d. Calcium-Silicate-Hydrates, Portlandite et Calcium-Silicate-Hydrates/Portlandite) à l'échelle nanométrique. Les silicates de calcium hydratés (C-S-H) et la Portlandite (CH) ont été choisis pour être étudiés car ils sont les principaux composants de la pâte de ciment hydraté durci. Les résultats pourraient nous amener à mieux comprendre les propriétés mécaniques et le comportement à la fissuration de la pâte de ciment hydraté. Pour conclure, il s'agit d'une autre étape pour étudier les propriétés mécaniques de la pâte de ciment à faible teneur en carbone, ce qui pourrait conduire à développer un ciment avec une meilleure résistance.

Abstract :

Nowadays, cement production is one of the main causes of carbon dioxide (CO_2) emission, which contributes to the cause of climate change. However, cement is still one of the main material for building construction because of the price, the ability to cast to different shape as the requirement of architecture and its strength. As a result, it is necessary to develop the strength of the hydrate cement paste. On one hand, it could involve in durability and sustainability of the structure. On the other hand, strength improvement could lead to less usage of cement, which also make it possible to reduce cement production. In order to response to this problem, the study of the mechanical properties of new cement pastes is very important, but it needs to improve knowledge at nanoscale. One of the method is by using molecular dynamics simulations. This method is quite popular in the study of mechanical properties of cement since it is tedious to perform the sample for experiment in such small scale. The homogenization of properties from nano-scale to micro-scale is not really mastered until now. In our study, we have performed the tensile tests using molecular dynamics simulation in order to find them for different components (i.e., Calcium-Silicate-Hydrates, Portlandite and Calcium-Silicate-Hydrates/Portlandite) at nano-scale. Calcium-Silicate-Hydrates (C-S-H) and Portlandite (CH) were chosen to investigate because they are the major components of hardened hydrated cement paste. The results could lead us to understand more clearly about the mechanical properties and cracking behaviour of hydrated cement paste. To conclude, it is another step to investigate the mechanical properties of low-carbon cement paste, which could lead to develop a cement with a better strength.

Keywords: Tensile test, cement paste phases, molecular dynamics, mechanical properties

1 Introduction

Concrete are by far the most used materials in the construction field and it is estimated that cement and concrete industry produce the global CO_2 emission for about 7-8% nowadays [10]. Concrete consists of a particulate phase (aggregates) and a binding phase (cement matrix) as a complex composite. As a result, the cement matrix affects the mechanical properties of concrete [15]. Cement paste is a porous multiscale substance with varying physical properties at different length scales [13]. Calcium-Silicate-Hydrate (C-S-H) is a major component of hardened hydrated cement paste, which occupies more than 50% volume in the paste [15]. Another major phase in hydrated cement is Portlandite ($Ca(OH)_2$) which occupies 20-25% of the volume fraction of the total mass [16].

With the advances in computational materials science and in the characterization of the nanoscale structure of cement-based materials, promising new tools make it possible for scientists and engineers understand and engineer better and improve concrete durability and performance [19]. To allow simulating precisely the behaviour of the concrete, for example to characterize its damage or cracking, it is necessary to develop the finest possible modelling of the cement paste and to ascend to the overall behaviour of the cementitious composite material. It is indeed the cement paste, which is the main responsible for this overall behaviour. However, this paste varies considerably with the chemistry and the fineness of the cement, the amount of water, the additions/admixtures ratio, the mixing procedure or the temperature. Any attempt to model concrete without taking into account the heterogeneity of the dough therefore requires systematic calibration of the mechanical properties of the latter, for example

through experiments. This harms the development of unconventional concrete based on industrial by-products for example, green-concrete.

However, all cement pastes share common characteristics influenced by two main elements: the component phases and the porous structures. Thus, it is now accepted that the objective of developing an advanced modelling tool will only be achieved by relying on nanostructure relationships - appropriate performances, the properties of the constituent phases of the cement paste and of the adhesion between these phases depending very much on the interatomic physicochemical bonds. This can be used within the framework of a performance-based formulation approach. This is why, more recently, the simulation methodology used in the work carried by certain members of the supervisory team has been extended to the scale of the crystal structure by means of Molecular Dynamics (MD) modelling or using Density Functional Theory (DFT), for instance, in thesis of Fu [7] and Claverie [2].

This paper aim to find the mechanical properties of main cement paste phases. Those phases are Calcium-Silicate-Hydrates, Portlandite, and Calcium-Silicate-Hydrate/Portlandite. The tensile test were performed using the Molecular Dynamics simulation with different strain rate (i.e., 10^{-4}/fs, 10^{-5}/fs and 10^{-6}/fs) and with two different force fields (i.e., ReaxFF and ClayFF). As a result, the stress-strain curves were obtained with the schemas of tensile test evolutions.

2 Materials and Methods

2.1 Microstructure of Hardened Cement Paste

The Portland cement produces the hydration products varied from coarsely crystalline Portlandite (CH) to almost amorphous C-S-H based on type [1]. For instance, in the case of a 14 months saturated old paste with w/c ratio of 0.5 obtained with a typical Portland cement hydrated, Taylor [20] calculated volume percentages based on the phase composition to be: Alite = 1%, Belite = 0.6%, Ferrite = 1%, insoluble residue = 1%, C-S-H = 48.7%, CH = 13.9%, AFm = 11.1%, AFt = 3.6%, Hydrogarnet = 2.2%, Hydrotalcite = 1.8% and pores = 16%. In proportion to the volume percentages of phase composition, two main phases are chosen to investigate (i.e., C-S-H and CH) in our study.

The C-S-H phases is often amorphous with no long-range order, while C-S-H structure is regarded to be similar to Tobermorite model mineral [8,21] if the Ca/Si ratio matches that of this model. Based on the ratio of Ca/Si, C-S-H phase can be grouped into calcium-rich and into silicon-rich forms [9] and can also be grouped into C-S-H (I) with Ca/Si ratio of 0.6-1.5 and C-S-H (II) with Ca/Si ratio of 1.5-2.0 [20]. C-S-H structures are most often modelled as Jennite-like systems [18] and as Tobermorite-like systems (i.e., Tobermorite 9, 11 and 14 Å) and/or with distorted semi-crystalline variations of them [14]. Both C-S-H (I) and C-S-H (II) structures resemble Tobermorite with the exception of which some silicon oxygen tetrahedrons in their silicon chain are partially lost or deformed and hence form some plurality of dimmers [3].

One of the possible ordered of the 11 Å natural Tobermorite structures is a monoclinic space group $P2_1$ with chemical formula ($Ca_4Si_6O_{14}(OH)_4 \cdot 2H_2O$) and with a = 6.69 Å, b = 7.39 Å, c = 22.779 Å and $\gamma = 123.49^0$ [12]. In the thesis of Fu [7], he developed C-S-H cell starting from Tobermorite 11 Å and obtained first amorphous Tobermorite whose long range is distorted. Following his procedure, we obtained the annealed amorphous structure.

As for Calcium Hydroxide or Portlandite, it is a trigonal crystal system ($P\bar{3}m1$) with a = b = 3.589 Å, c = 4.911 Å, V = 54.8 $Å^3$ and D_x = 2.26 g cm^{-3} at room temperature. The unit cell of Portlandite (CH) was modelled following Desgranges et al. [5]. It has chemical formula: $Ca(OH)_2$ and cell angles (α, β, γ) = (90^0 , 90^0 , 120^0).

2.2 Force Field

Force field is very important in the simulation of Molecular Dynamics (MD) and there are multiple force fields. For instance, Clay Force Field (ClayFF) which is a Classical Molecular Dynamics (CMD) and Reactive Force Field (ReaxFF) which is a Reactive Molecular Dynamics (RMD). For ClayFF, it works with CH and C-S-H, whereas ReaxFF works with CH, C-S-H and Sulfoaluminate (AFm, AFt). In order to run ClayFF in LAMMPS, bonds between atoms are created in the beginning of the simulation. For ReaxFF, it is not required to create bonds between atoms at the start of simulation. However, ReaxFF is time consuming compared to ClayFF. In our study, ReaxFF is chosen for the tensile test with MD for the case of C-S-H (I) and C-S-H (I)/CH supercells whereas ClayFF was applied on CH supercells.

Van Duin et al. [6] developed ReaxFF (Reactive Force Field for Hydrocarbons) which is a force field for reactive systems in order to make practical the molecular dynamics simulation of large scale reactive chemical systems. On one hand, ReaxFF uses a general relationship between bond order and bond distance. On the other hand, ReaxFF uses a general relationship between bond order and bond energy which leads to proper dissociation of bonds to separated atoms. Other valence terms that present in the force field (torsion and angle) are defined in terms of the same bond orders. Thus, all these terms go to zero smoothly as bond break. Moreover, to describe non-bond interactions between all atoms (no exclusions), Morse (van der Waals) and Coulomb potentials are also included in ReaxFF. From reactions of small molecules plus geometry data and heat of formation for a number of stable hydrocarbon compounds and quantum chemical calculations on bond dissociation, the parameters were derived. The classical force fields are unable to describe the chemical reactions, which will be initiated because of large deformations. This matter has been taken into account in the study of Hajilar and Shafei [11] through RMD simulations using ReaxFF. The harmonic bonds of classical MD is substituted by the bond orders and energies based on interatomic distances. With this approach, it is capable of capture the bond breakage and formation while the bonded interactions are permitted to decay smoothly to zero. For all the atoms in the system by a screened taper function, the van der Waals and non-bonded Columbic interactions are calculated. The charged equilibrium (Q_{Eq}) method determines the atomic charges and need to be updated at every time step. The parameters of ReaxFF can be found from Liu et al. [17]. The ReaxFF divides the system energy up into various partial energy contributions similarly to empirical non-reactive force fields as shown in **Eq. 1** [6].

$$E_{system} = E_{bond} + E_{over} + E_{under} + E_{val} + E_{pen} + E_{tors} + E_{conj} + E_{vdWaals} + E_{Coulomb} \quad (1)$$

where E_{bond} is bond energy, E_{over} and E_{under} are energy penalty for over- and under-coordination of atoms, E_{val}, E_{pen}, E_{tors}, E_{conj}, $E_{vdwaals}$ and $E_{couloumb}$ are valence angle, penalty, torsion, conjugation, van der Waals and Coulombic energy, respectively.

In the paper of Cygan et al. [4], they demonstrate an alternative approach to develop a general force field for molecular simulation of hydrated crystalline compounds and their interfaces with fluid phases and ClayFF is based on a non-bonded (ionic) description of the metal-oxygen interactions which is

associated with hydrated phases. Within this force field framework, all atom are represented as point charges and are allowed to complete translational freedom. Metal-oxygen interactions are based on a simple Lennard-Jones (12-6) potential combining with electrostatics. The results of Cygan et al. [4] show that ClayFF force field has a good promise to be usable into a widely adaptable and broadly effective force field for simulations of molecular of fluid interfaces with other clay-related phases and clays, as well as other inorganic materials defined by complex, disordered, and often composition and ill-determined structure.

The total energy has contribution from the Coulombic interactions, the van der Waals interaction, bond stretch and angle bend interactions [4]:

$$E_{total} = E_{Coul} + E_{vdW} + E_{bond\ stetch} + E_{angle\ bend} \quad (2)$$

where $E_{Coul}, E_{vdW}, E_{bond\ stretch}$ and E_{val} are Coulombic, van der Waals, bond stretch, and angle bend energy, respectively.

2.3 Procedure

Firstly, each individual supercell was gotten from the replication in x, y and z directions, respectively and then changing the cell from triclinic to orthogonal cell. It was simulated in three dimensions and real units with periodic boundary condition along three dimensions. Secondly, the random velocity were set to the supercell with the temperature of 300 K. After that, an energy minimization of the system was performed. Thirdly, they were relaxed in the NPT ensemble with the pressure of 0 atm along x, y and z directions and with temperature of 300 K for 50 ps. Finally, the relaxed supercells were deformed along z direction while the NPT ensemble with the pressure of 0 atm and with temperature of 300 K were set to perpendicular directions. In order to see the effect of strain rate, the strain rates are set to 10^{-4}/fs, 10^{-5}/fs and 10^{-6}/fs with supercells of CH and C-S-H (I).

Similarly, C-S-H (I)/CH composite tensile test with ReaxFF force field was done following the same procedure. To get the two supercells with similar size, the CH and C-S-H (I) unit cell are replicated 9 × 10 × 14 and 5 × 5 × 3 along x, y and z directions, respectively. C-S-H (I) and CH supercells were first minimized and relaxed individually with 300 K in NPT ensemble for 50 ps. Then, they were put together as composite with CH supercell on top of C-S-H (I) supercell and the 1 Å vacuum spacing or 3.1 Å/6.2 Å water spacing in between them in other cases. After that, the C-S-H (I)/CH composite was minimized and relaxed again with NPT ensemble for another 50 ps. Finally, tensile test with strain rate of 10^{-6}/fs was applied along y/z directions while the NPT ensemble with the pressure of 0 atm and with temperature of 300 K were set to perpendicular directions.

3 Results

3.1 C-S-H (I) Tensile Test with ReaxFF

In the first case, we have used the annealed amorphous supercells of C-S-H (I) which are replicated in x, y and z directions to 5×5×3 from the unit cell. ReaxFF force field was applied on this supercell. **Fig. 1a** shows the stress-strain curves with three different strain rates. It could be seen clearly that the strain rate have effect on the stress-strain curves of supercell C-S-H (I).

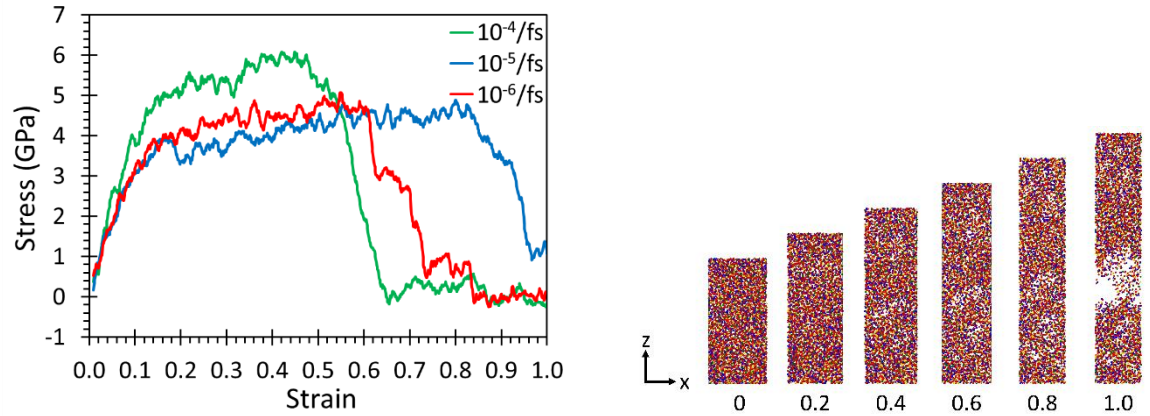

(a) (b)

Figure 1: *Stress-strain curves of three different strain rates and tensile evolutions of 10^{-5}/fs strain rate of supercell C-S-H (I) 5×5×3 (Green balls are calcium atoms (Ca); yellow balls are silicon atoms (Si); red balls are oxygen atoms (O); blue balls are hydrogen atoms (H).)*

As shown in **Fig. 1b**, the rupture is initiated at around the middle of simulation box. These simulations were run parallel with 8 processors on CPU Intel Xeon Gold @2.2 GHz and 64 GB of RAM. The file sizes of each simulation is 665.2 MB and time comsuming ranging from about 48 to 206 hours.

3.2 CH Tensile Test with ClayFF

In the second case, we have used CH supercells which are replicated in x, y and z directions to 10×10×10 from the unit cell. The simulations of CH supercells were running with the ClayFF force field. As shown in **Fig. 2a**, it could be seen that the stresses return to the value of around 0 GPa immediately after reaching the peak stress for the strain rate of 10^{-5}/fs and 10^{-6}/fs. This means that behavior of strain-strain curves seem to be more fragile with smaller strain rate.

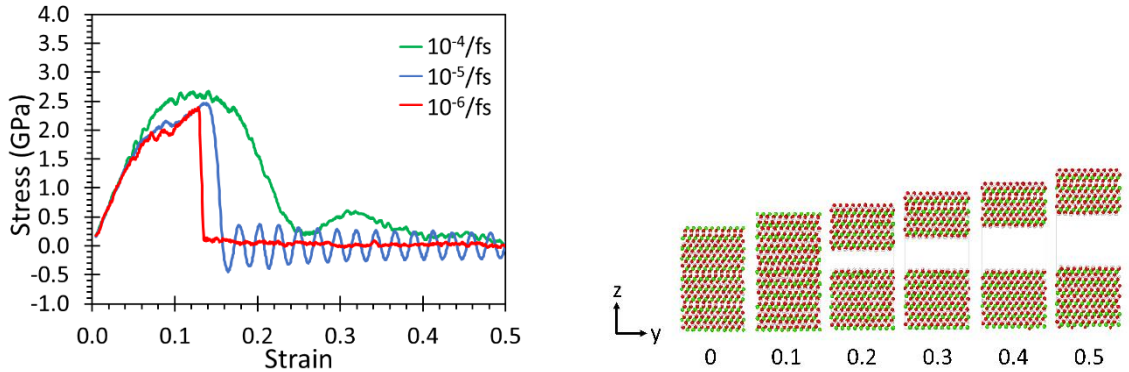

(a) (b)

Figure 2: *Stress-strain curves of three different strain rates and tensile evolutions of 10^{-5}/fs strain rate of supercell CH 10×10×10 (Lime balls are calcium atoms (Ca); white balls are hydrogen atoms (H); red balls are oxygen atoms (O).)*

Fig. 2b shows the tensile evolutions of CH supercell 10×10×10 at strain rate of 10^{-5}/fs with a rupture at the middle of the simulation boxes. The simulations were run parrallel with 2 processors for strain rate of 10^{-4}/fs and 10^{-5}/fs and with 4 processors for strain rate of 10^{-6}/fs on CPU Intel Core i7-8700T @2.4 GHz and 8 GB of RAM. The file size is 693 MB with time consumming ranging from about 6 to 32 hours.

3.3 C-S-H(I)/CH Tensile Test with ReaxFF

In the last case, 9×10×14 CH supercell was placed on top of 5×5×3 C-S-H (I) supercell with three different cases which are 1Å vacuum spacing, 3.1 Å water spacing and 6.2 Å water spacing between them. ReaxFF force field is used on these supercells. **Fig. 3** shows that the peak stress along the y direction is bigger than the z direction for vacuum spacing. Nontheless, 3.1 Å and 6.2 Å water spacing simulations provides similar peak stress values.

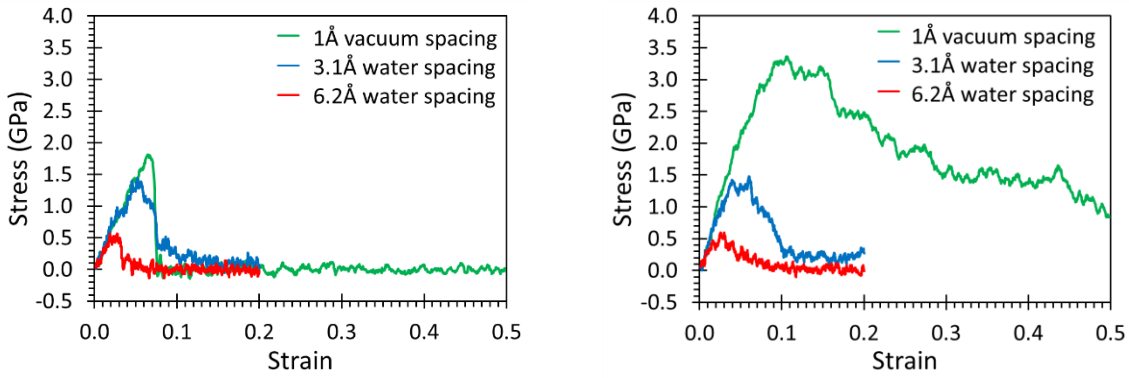

(a) deformation along z direction (b) deformation along y direction

Figure 3: *Stress-strain curve of three different cases of C-S-H (I)/CH composite*

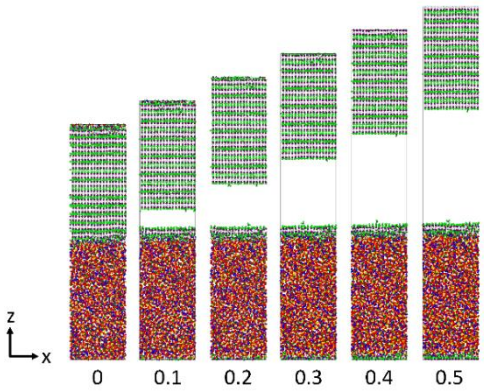

(a) 1Å vacuum spacing

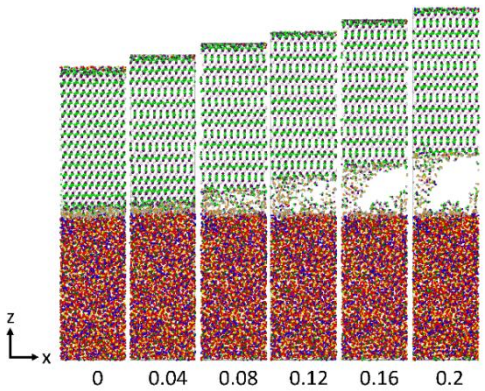

(b) 3.1Å water spacing

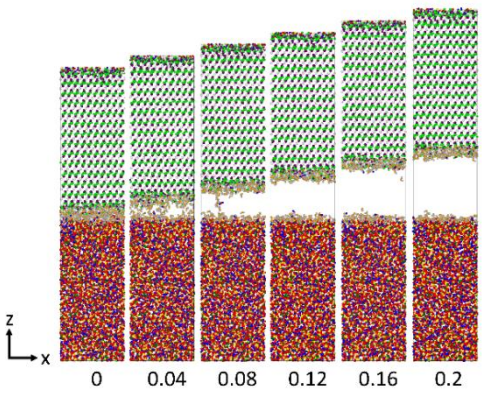

(c) 6.2Å water spacing

Figure 4: *Tensile test evolution of three different cases of C-S-H (I)/CH composite (In C-S-H (I) phase at lower part; green balls are calcium atoms (Ca); yellow balls are silicon atoms (Si); red balls are*

oxygen atoms (O); blue balls are hydrogen atoms (H). In CH phase at the upper part, white balls are calcium atoms (Ca); lime balls are hydrogen atoms (H); purple balls are oxygen atoms (O). In water between them, silver balls are hydrogen atoms (H); orange balls are oxygen atoms (O).)

As shown in **Fig. 4**, the rupture along z direction happens into the phase of CH with spacing of vacuum and the ruptures occur at the interface between the C-S-H (I) and CH with water in between them. It should be notice that these simulations are time consuming and it could last longer if we choose to simulate on a lower performance computer. These simulations were executed parallel with 16 processors on CPU Intel Xeon Gold @2.2 GHz and 64 GB of RAM. The running time and file size are ranged from about 54 to 130 hours and from around 243 to 293 MB, respectively.

4 Conclusion

In conclusion, the cement paste phases of C-S-H (I) and CH were applied to three different strain rates (i.e., 10^{-4}/fs, 10^{-5}/fs and 10^{-6}/fs). We have found that the strain rates have effect on the stress-strain curve that lead to variety of peak stress and peak strain values. For the C-S-H (I)/CH composite, the rupture is happened into the phase of CH for the case of 1 Å vacuum spacing and at the interface in the cases of 3.1 Å /6.2 Å water spacing between them.

References

[1] G. Bye, The hydration of Portland cement, in: Portland Cement: Third Edition, ICE Publishing, 2011: pp. 89–121.
[2] J. Claverie, Molecular dynamics investigation of the mechanical, thermal and surface properties of tricalcium silicate and its early hydration, Universidade Estadual Paulista (Unesp), 2019.
[3] X. Cong, R.J. Kirkpatrick, 29Si MAS NMR study of the structure of calcium silicate hydrate, Advanced Cement Based Materials. 3 (1996) 144–156.
[4] R.T. Cygan, J.-J. Liang, A.G. Kalinichev, Molecular Models of Hydroxide, Oxyhydroxide, and Clay Phases and the Development of a General Force Field, J. Phys. Chem. B. 108 (2004) 1255–1266.
[5] L. Desgranges, D. Grebille, G. Calvarin, G. Chevrier, N. Floquet, J.-C. Niepce, Hydrogen thermal motion in calcium hydroxide: $Ca(OH)_2$, Acta Cryst B. 49 (1993) 812–817.
[6] A.C.T. van Duin, S. Dasgupta, F. Lorant, W.A. Goddard, ReaxFF: A Reactive Force Field for Hydrocarbons, J. Phys. Chem. A. 105 (2001) 9396–9409.
[7] J. Fu, Multiscale modeling and mechanical properties of typical anisotropic crystals structures at nanoscale, These en préparation, Rennes, INSA, 2016.
[8] S. Grangeon, F. Claret, C. Lerouge, F. Warmont, T. Sato, S. Anraku, C. Numako, Y. Linard, B. Lanson, On the nature of structural disorder in calcium silicate hydrates with a calcium/silicon ratio similar to tobermorite, Cement and Concrete Research. 52 (2013) 31–37.
[9] M.W. Grutzeck, J. LaRosa-Thompson, S. Kwan, Characteristics of CSH gels, in: Proceedings 10th International Congress on the Chemistry of Cement, Gothenburg, Sweden, Amarkai AB and Congrex Göteborg AB, Göteborg, Sweden, 1997.
[10] P. Hajek, Concrete Structures for Sustainability in a Changing World, Procedia Engineering. 171 (2017) 207–214.
[11] S. Hajilar, B. Shafei, Mechanical failure mechanisms of hydrated products of tricalcium aluminate: A reactive molecular dynamics study, Materials & Design. 90 (2016) 165–176.
[12] S.A. Hamid, The crystal structure of the 11Å natural tobermorite $Ca_{2.25}[Si_3O_{7.5}(OH)_{1.5}] \cdot 1H_2O$, Zeitschrift Für Kristallographie - Crystalline Materials. 154 (1981) 189–198.

[13] K. Ioannidou, Mesoscale Structure and Mechanics of C-S-H, in: W. Andreoni, S. Yip (Eds.), Handbook of Materials Modeling: Applications: Current and Emerging Materials, Springer International Publishing, Cham, 2020: pp. 1–15.
[14] S. Kwan, J. LaRosa-Thompson, M.W. Grutzeck, Structures and Phase Relations of Aluminum-Substituted Calcium Silicate Hydrate, Journal of the American Ceramic Society. 79 (1996) 967–971.
[15] D. Lau, W. Jian, Z. Yu, D. Hui, Nano-engineering of construction materials using molecular dynamics simulations: Prospects and challenges, Composites Part B: Engineering. 143 (2018) 282–291.
[16] J.L. Laugesen, Density functional calculations of elastic properties of portlandite, $Ca(OH)_2$, Cement and Concrete Research. 35 (2005) 199–202.
[17] L. Liu, A. Jaramillo-Botero, W.A. Goddard, H. Sun, Development of a ReaxFF Reactive Force Field for Ettringite and Study of its Mechanical Failure Modes from Reactive Dynamics Simulations, J. Phys. Chem. A. 116 (2012) 3918–3925.
[18] L. Raki, J. Beaudoin, R. Alizadeh, J. Makar, T. Sato, Cement and Concrete Nanoscience and Nanotechnology, Materials. 3 (2010) 918–942.
[19] F. Sanchez, K. Sobolev, Nanotechnology in concrete – A review, Construction and Building Materials. 24 (2010) 2060–2071.
[20] H.F.W. Taylor, Cement chemistry, 2. ed., Repr, Telford, London, 1997.
[21] H.F.W. Taylor, J.W. Howison, Relationships between calcium silicates and clay minerals, Clay Minerals Bulletin. 3 (1956) 98–111.